Polymer 50 (2009) 4089–4100

Contents lists available at ScienceDirect

Polymer

journal homepage: www.elsevier.com/locate/polymer

Morphology and mechanical properties of nanostructured blends of epoxy resin with poly(ε-caprolactone)-*block*-poly(butadiene-*co*-acrylonitrile)-*block*-poly(ε-caprolactone) triblock copolymer

Xingtian Yang [a], Fangping Yi [a], Zhirong Xin [b], Sixun Zheng [a,*]

[a] *Department of Polymer Science and Engineering and State Key Laboratory of Metal Matrix Composites, Shanghai Jiao Tong University, Shanghai 200240, PR China*
[b] *College of Chemistry and Biology, Yantai University, Shandong 264005, PR China*

ARTICLE INFO

Article history:
Received 17 March 2009
Received in revised form
28 May 2009
Accepted 15 June 2009
Available online 21 June 2009

Keywords:
Epoxy
Poly(ε-caprolactone)-*block*-poly(butadiene-*co*-acrylonitrile)-*block*-poly(ε-caprolactone) triblock copolymer
Reaction-induced microphase separation

ABSTRACT

Poly(ε-caprolactone)-*block*-poly(butadiene-*co*-acrylonitrile)-*block*-poly(ε-caprolactone) triblock copolymer was synthesized *via* the ring-opening polymerization of ε-caprolactone with dihydroxyl-terminated butadiene-*co*-acrylonitrile random copolymer. The amphiphilic block copolymer was used to toughen epoxy thermosets *via* the formation of nanostructures. The morphology of the thermosets was investigated by means of atomic force microscopy, transmission electronic microscopy and small-angle X-ray scattering. It was judged that the formation of the nanostructures in the thermosets follows the mechanism of reaction-induced microphase separation. The thermal and mechanical properties of the nanostructured thermosets were compared to those of the ternary blends composed of epoxy, poly(butadiene-*co*-acrylonitrile) and poly(ε-caprolactone) with the identical content of the modifiers. It is noted that at the same composition the nanostructured thermosets displayed higher glass transition temperatures (T_gs) than the ternary blends, which was evidenced by dynamic mechanical analysis. The fracture toughness of the thermosets was evaluated in terms of the measurement of critical stress field intensity factor (K_{1C}). It is noted that at the identical composition the nanostructured blends significantly displayed higher fracture toughness than the ternary blends. In addition, the K_{1C} of the nanostructured thermosets attained the maximum with the content of the modifier less than their counterpart of ternary blending.

1. Introduction

Thermosets such as epoxy and novolac resins are a class of important polymeric materials and have widely been used as high performance materials such as adhesives, matrices of composites and electronic encapsulating materials. However, these materials are inherently of low impact resistance due to their high crosslinking density. During the past decades considerable efforts have been done to improve toughness of epoxy thermosets [1–21]. One of the successful routines is to incorporate polymeric modifiers into thermosetting matrix to form fine phase-separated morphology; these polymeric modifiers can be either elastomers or thermoplastics. Generally, the modified thermosets are prepared starting from the homogeneous solution composed of precursors of thermosets and the modifiers; reaction-induced demixing takes place with curing reaction proceeding [20]. The reaction-induced phase separation generally occurs on the macroscopic scale since these modifiers are some homopolymers or random copolymers. The fine heterogeneous morphology is crucial for the improvement of toughness in terms of several known toughening mechanisms such as shear yielding [3,4,21], particle bridging [22], crack-pinning [23] and microcracking mechanisms [24,25]. Recently, it has been recognized that the formation of nanostructures in multi-component thermosets can further optimize the interactions between thermosetting matrix and modifiers and thus the mechanical properties of materials were significantly improved, which has been called "toughening by nanostructures" [26]. However, such a study remains largely unexplored.

The control of the formation of nanostructures in thermosets using block copolymers has recently provoked considerable interests [27–52]. It has been identified that the formation of the nanostructures could follow either self-assembly [27,28] or reaction-induced microphase separation mechanism [29,30]. Bates et al. [27,28] have first reported the strategy of creating nanostructures *via* self-assembly approach. In the protocol, the precursors of thermosets act as the selective solvents of block copolymers and some

* Corresponding author. Tel.: +86 21 54743278; fax: +86 21 54741297.
E-mail address: szheng@sjtu.edu.cn (S. Zheng).

0032-3861/$ – see front matter © 2009 Elsevier Ltd. All rights reserved.
doi:10.1016/j.polymer.2009.06.030

self-assembly nanostructures such as lamellar, bicontinuous, cylindrical, and spherical structures are formed in the mixtures depending on the blend composition before curing reaction. These nanostructures can be further fixed *via* subsequent curing with introduction of hardeners. With an appropriate design of block copolymer architecture, the block copolymers self-organize to form ordered or disordered nanostructures [27,28]. More recently, it was reported that ordered or disordered nanostructures in thermosets can be alternatively accessed *via* reaction-induced microphase separation (RIMS) mechanism [29,30]. In this mechanism, a part of subchains of the block copolymers were demixed with the occurrence of polymerization whereas the other subchains still remain miscible with the matrix of the thermosets.

During the past years there have been a lot of reports on the formation of a variety of nanostructures in thermosets [27–52], nonetheless, only a few of them are concerned with the studies on fracture mechanics of nanostructured thermosets [37,50–52]. Bates et al. [50–52] have investigated the effect of various nanostructures such as micelle, vesicles or wormlike vesicles and found that the toughening of nanostructured thermosets are quite dependent on type and shape of dispersed nanophase and the interactions of the nanophases with thermosetting matrix, which could significantly affect either the debonding of the nanodomains (*i.e.*, micelle or vesicles) from thermosetting matrix or crack deflection and frictional interlocking for the thermosets possessing the terraced morphology [52]. Pascault and Leibler et al. [37] have reported maximum critical stress field intensity factors (*i.e.*, K_{1C}) improvement of around two times by particles forming the 'sphere-on-sphere' nanostructures in epoxy thermosets. It is of importance to investigate the effect of nanostructures in thermosets on thermomechanical properties such as glass transition behavior and fracture toughness compared to the macroscopically-heterogeneous blends of thermosets with the identical composition.

In this work, we present a comparative investigation on the thermomechanical properties of microphase- and macrophase-separated blends of epoxy thermosets. Toward this end, an amphiphilic triblock copolymer, poly(ε-caprolactone)-*block*-poly(butadiene-*co*-acrylonitrile)-*block*-poly(ε-caprolactone) (PCL-*b*-PBN-*b*-PCL) was synthesized. The design of the block copolymers is based on the knowledge that PCL is miscible with epoxy thermosets after and before curing reaction [53,54] whereas PBN will undergo reaction-induced phase separation in its blends with epoxy resin [1,3,5,9]. It is expected that the nanostructured epoxy thermosets can be prepared *via* reaction-induced microphase separation in this system. In the meantime, the ternary blends of epoxy resin with poly(butadiene-*co*-acrylonitrile) and poly(ε-caprolactone) with the identical composition with the above nanostructured blends were also prepared. The morphology of the above two systems was investigated by means of transmission electronic microscopy (TEM), atomic force microscopy (AFM) and small-angle X-ray scattering (SAXS). The fracture toughness was addressed on the basis of the measurements of critical stress intensity factors (K_{IC}) of the materials.

2. Experimental

2.1. Materials

Diglycidyl ether of bisphenol A (DGEBA) with epoxide equivalent weight of 185–210 was purchased from Shanghai Resin Co., China. The curing agent is 4,4′-methylenebis-(2-chloroaniline) (MOCA), supplied by Shanghai Reagent Co., China. The monomer, ε-caprolactone (ε-CL), was purchased from Fluka Co., Germany and it was distilled over calcium hydride (CaH_2) under decreased pressure prior to polymerization. Stannous octanoate [$Sn(Oct)_2$] was of analytical grade, purchased from Aldrich Co., USA and used as received. The hydroxyl-terminated butadiene-*co*-acrylonitrile random copolymer (HTBN) was kindly supplied by Qilong Chemical Company, Shandong, China and the content of acrylonitrile in the copolymer is about 10 wt% and it has a quoted molecular weight to be $M_n = 2500$. Before use, HTBN was dried by an azeotropic distillation using anhydrous toluene.

2.2. Synthesis of PCL-b-PBN-b-PCL triblock copolymer

Poly(ε-caprolactone)-*block*-poly(butadiene-*co*-acrylonitrile)-*block*-poly(ε-caprolactone) triblock copolymer (PCL-*b*-PBN-*b*-PCL) was synthesized *via* the ring-opening polymerization of ε-CL in the presence of HTBN with stannous octanoate [$Sn(Oct)_2$] as the catalyst. Prior to polymerization, all the glassware was carefully dried at 150 °C for 3 h and then *in vacuo* to ensure the waterless system. The synthesis was carried out on a standard Schlenk line system. Typically, to a round-bottom flask equipped with a dried magnetic stirrer, HTBN (1.800 g, 1.44 mmol of hydroxyls) and ε-CL (3.600 g, 31.5 mmol) were charged and $Sn(Oct)_2$ [1/1000 (wt) with respect to the mass of ε-CL] dissolved in anhydrous toluene was added using a syringe. The reactive mixture was degassed *via* three pump–freeze–thaw cycles and then immersed in a thermostated oil bath at 130 °C. The polymerization was carried out at 130 °C with for 30 h. The crude product was dissolved in THF and precipitated with a great amount of diethylether and this procedure was repeated three times to purify the samples. The resulting polymer was dried in a vacuum oven at 40 °C for 48 h prior to use. The polymer (5.245 g) was obtained with the yield (or conversion of ε-CL) of >97%. The measurement of gel permeation chromatography (GPC) gives the molecular weight of the triblock copolymer to be: $M_n = 9100$ with $M_w/M_n = 1.32$.

2.3. Synthesis of model PCL

The model PCL homopolymers having the identical molecular weight with the length of the PCL block in the triblock copolymer was synthesized *via* the ring-opening polymerization of ε-CL with benzyl alcohol as the initiator and stannous octanoate [$Sn(Oct)_2$] as the catalyst. Typically, to a round-bottom flask equipped with a dried magnetic stirrer benzyl alcohol (0.7000 g, 6.5 mmol hydroxyls) and ε-CL (15.2000 g, 133.3 mmol) were charged and $Sn(Oct)_2$ (1/1000 wt with respect to the mass of ε-CL) dissolved in anhydrous toluene was added. The reactive mixture was degassed *via* three pump–freeze–thaw cycles and then immersed in a thermostated oil bath at 130 °C, at which the polymerization was carried out for 30 h. The crude product was dissolved in THF and dropped into a great amount of diethylether to obtain the precipitate. The procedure was repeated three times to purify the sample. The resultant polymer was dried in a vacuum oven at 40 °C for 48 h prior to use. The polymer (15.602 g) was obtained with the yield (or conversion of ε-CL) of >98%. The molecular weight was determined by means of ^{1}H NMR spectroscopy and was calculated according to the ratio of integration intensity of aliphatic methylene protons to aromatic protons to be $M_n = 2600$.

2.4. Preparation of thermosets

The samples of DGEBA/HTBN blends for the measurement of cloud point curve were prepared *via* solution casting technique. The pre-weighted DGEBA and HTBN were mixed with tetrahydrofuran (THF) as the co-solvent. The concentration was controlled within 5% (w/v). The majority of solvent was evaporated at room temperature and the residual solvent was eliminated *in vacuo* at 50 °C for 48 h. The desired amount of DGEBA and PCL-*b*-PBN-*b*-PCL was mixed at 100 °C with vigorous stirring and the curing agent (*i.e.*, MOCA) was added with continuous

stirring until transparent and homogenous mixtures were obtained. The mixtures were poured into Teflon moulds and subjected to the thermal curing at 150 °C for 4 h. The thermosets containing PCL-*b*-PBN-*b*-PCL up to 40 wt% were prepared. The similar procedures were also applied to the preparation of the ternary blends of epoxy thermosets, HTBN and PCL. The contents of PBN and PCL were controlled to be identical with those in the thermosetting blends containing PCL-*b*-PBN-*b*-PCL triblock copolymer. The same curing conditions were applied to obtain the ternary blends of epoxy thermoset with PBN and PCL.

2.5. Measurement and characterization

2.5.1. Fourier transform infrared (FTIR) spectroscopy

The FTIR measurements were conducted on a Perkin–Elmer Paragon 1000 Fourier transform spectrometer at room temperature (25 °C). The block copolymer was dissolved with THF (10 wt%) and the solution was cast onto KBr windows. The solvent was eliminated in a vacuum oven at 60 °C for 30 min. The specimens of thermosets were granulated and the powder was mixed with KBr pellets to press into the small disks for measurements. All the specimens were sufficiently thin to be within a range where the Beer–Lambert law is obeyed. In all cases 64 scans at a resolution of 2 cm^{-1} were used to record the spectra.

2.5.2. Nuclear magnetic resonance (NMR) spectroscopy

The NMR measurements were carried out on a Varian Mercury Plus 400 MHz NMR spectrometer at 25 °C. The samples were dissolved with deuterated chloroform and the solutions were measured with tetramethylsilane (TMS) as the internal reference.

2.5.3. Gel permeation chromatography (GPC)

The molecular weights of the polymers were measured on a Perkin–Elmer 200 GPC instrument with a PL mixed-B10m column and a reflective index detector. Polystyrene was used as the standard, and *N*,*N*-dimethylformamide (DMF) was used as the eluent at a flow rate of 1 mL/min.

2.5.4. Phase contrast microscopy (PCM)

A Leica DMLP polarized optical microscope equipped with a hot stage (Linkam TH960, Linkam Scientific Instruments, Ltd., UK) with a precision of ±0.1 °C was used for the determination of cloud point curve of DGEBA/HTBN mixtures. The THF solutions of the mixtures were cast onto cover glasses; the major of solvent was removed at 50 °C and the residual solvent was further eliminated by drying the samples *in vacuo* at 50 °C for 2 h. The films of the blends were sandwiched between two cover glasses. For measurements of cloud point curve (CPC), the blend films with various compositions were observed under the polarizing microscope in which the angle between the polarizer and analyzer was 45° [55]. The samples were heated through the cloud points at the rate of 5 °C/min, and the cloud point was defined as the onset of the turbidity. The cloud points were plotted as a function of blend composition.

2.5.5. Differential scanning calorimetry (DSC)

The calorimetric measurements were performed on a Perkin–Elmer Pyris 1 differential scanning calorimeter in a dry nitrogen atmosphere. An indium standard was used for temperature and enthalpy calibrations, respectively. The samples (about 8.0 mg in weight) were first heated to 180 °C and held at this temperature for 3 min to remove the thermal history, followed by quenching to −60 °C. A heating rate of 20 °C/min was used at all cases. Glass transition temperature (T_g) was taken as the midpoint of heat capacity change. The crystallization temperatures (T_c) and the melting temperatures (T_m) were taken as the temperatures of the minimum and the maximum of both endothermic and exothermic peaks, respectively.

2.5.6. Small-angle X-ray scattering (SAXS)

The SAXS measurements were taken on a Bruker Nanostar small-angle X-ray scattering system. Two-dimensional diffraction patterns were recorded using an image intensified CCD detector. The experiments were carried out at room temperature (25 °C) or elevated temperature using Cu K radiation ($\lambda = 1.54$ Å, wavelength) operating at 40 kV, 35 mA. The intensity profiles were output as the plot of scattering intensity (I) *versus* scattering vector, $q = (4\pi/\lambda)\sin(\theta/2)$ (θ is the scattering angle).

2.5.7. Scanning electronic microscope (SEM)

In order to observe the phase structure of epoxy blends, the samples were fractured under cryogenic condition using liquid nitrogen. The fractured surfaces so obtained were immersed in tetrahydrofuran at room temperature for 30 min. The HTBN phases could be preferentially rinsed with the solvent while epoxy matrix phase remains unaffected. The etched specimens were dried to remove the solvents. The fracture surfaces were coated with thin layers of gold of about 100 Å. All specimens were examined with an Hitachi S210 scanning electron microscope (SEM) at an activation voltage of 15 kV.

2.5.8. Transmission electron microscopy (TEM)

Transmission electron microscopy (TEM) was performed on a JEOL JEM-2010 high-resolution transmission electron microscope at an acceleration voltage of 120 kV. The samples were trimmed using a microtome machine and the section samples were stained with O_SO_4 to increase the contrast. The stained specimen sections (*ca.*, 70 nm in thickness) were placed in 200 mesh copper grids for observations.

2.5.9. Atomic force microscopy (AFM)

The AFM experiments were performed with a Nanoscope IIIa scanning probe microscope (Digital Instruments, Santa Barbara, CA). Tapping mode was employed in air using a tip fabricated from silicon (125 μm in length with *ca.* 300 kHz resonant frequency). Typical scan speeds during recording were 0.3–1 line × s^{-1} using scan heads with a maximum range of 16 × 16 μm.

2.6. Fracture toughness measurements

Fracture toughness was measured by the notched three-point bending test with a crosshead speed of 1.3 mm^{-1} according to the standard of ASTM E399. The schematic diagram of the three-point bending specimens is shown in Scheme 1. The critical stress intensity factors (K_{IC}) were calculated using the following equation:

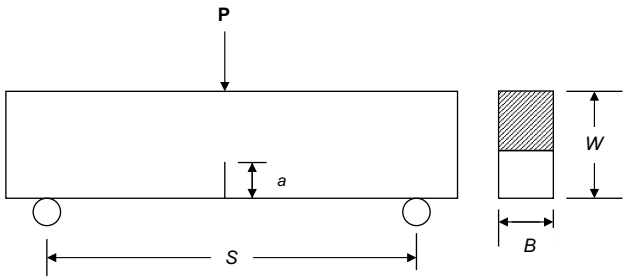

Scheme 1. Schematic diagram of three-point bending specimen for the measurement of critical stress intensity factor (K_{1C}).

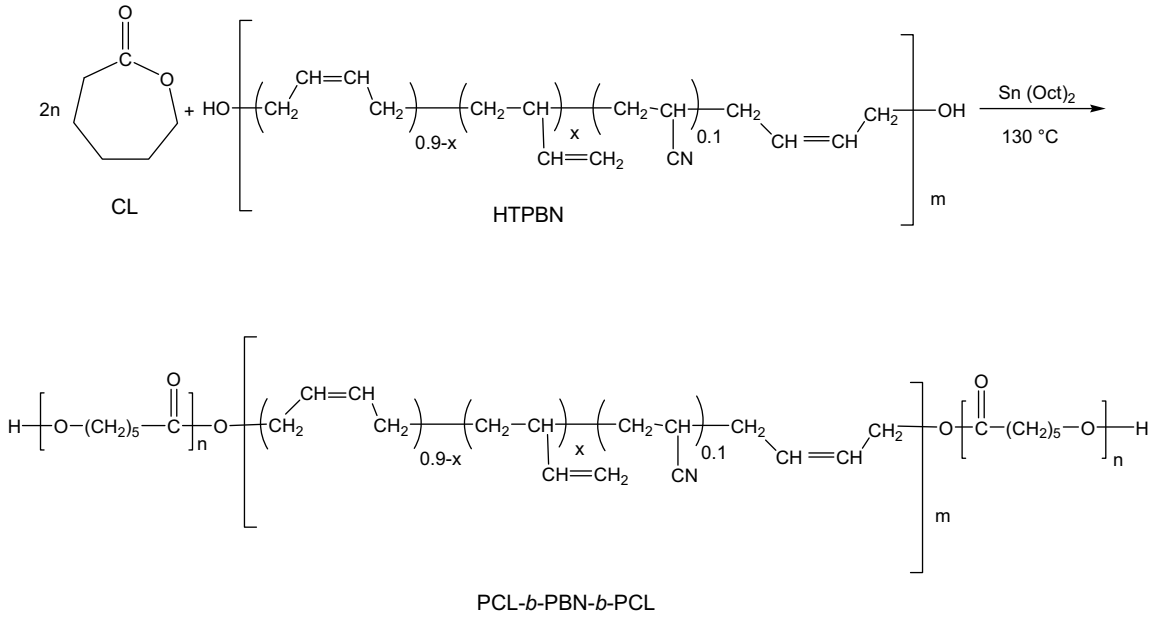

Scheme 2. Synthesis of PCL-*b*-PBN-*b*-PCL triblock copolymer.

$$K_{IC} = P_C S/BW^{3/2} f\left(\frac{a}{W}\right) \quad (1)$$

where P_C is the load at crack initiation, B is the thickness of the specimens, S is the span width, W is the width of the specimens and a is the crack length. Before measurement, all the specimens were annealed at 80 °C for 24 h and at least 5 successful measurements were used to obtain the average values of the measurements.

3. Results and discussion

3.1. Synthesis of PCL-b-PBN-b-PCL triblock copolymer

The PCL-*b*-PBN-*b*-PCL triblock copolymer was synthesized *via* the ring-opening polymerization of ε-CL with liquid dihydroxyl-terminated butadiene-*co*-acrylonitrile elastomer (HTBN) as the initiator and stannous octanoate [$Sn(Oct)_2$] was used as the catalyst as shown in Scheme 2. The polymerization was carried out at 130 °C for 30 h. The FTIR spectrum of the product is shown in Fig. 1. The ester carbonyls (>C=O) of PCL are characteristic of the stretching vibration at *ca.* 1728 cm^{-1}; the absorption bands at *ca.* 2943 cm^{-1} indicate the presence of methylene ($-CH_2-$) moieties in PCL subchains, assignable to the stretching vibration of C–H bonds. The band at 2237 cm^{-1} is attributed to the stretching vibration of –CN group in PBN. The bands at 967 and 730 cm^{-1} are ascribed to the out-of-plane bending vibration of =C–H bonds in *trans*-1,4 and *cis*-1,4 moieties in PBN blocks, respectively; the weak absorption at 911 cm^{-1} is attributed to the out-of-plane bending vibration of 1,2-structures in the PBN subchains. The spectral results indicate that the resulting polymer combined the structural features from both PCL and PBN. The molecular weight of the triblock copolymer can be estimated by means of ^{1}H NMR spectroscopy. The ^{1}H NMR spectrum of the copolymer is shown in Fig. 2. The resonances of protons from PCL and PBN blocks are indicated in this spectrum. In term of the ratio of integration intensity of the terminal hydroxy-methylene proton ($-C\mathbf{H_2}-OH$, $\delta = 3.86$ ppm) to other methylene protons of PCL, the length of PCL can be calculated to be $M_n \approx 2600$. According to the length of PCL, the overall molecular weight of the triblock copolymer was estimated to be $M_n = 7700$, which is in a good agreement with the value predicted with the feed ratio. The molecular weight of triblock copolymer was further measured by means of gel permeation chromatography (GPC) and the polymer exhibits a unimodal distribution of molecular weights with $M_n = 9100$ and $M_w/M_n = 1.32$. The quite narrow distribution of molecular weight indicates that the ring-opening polymerization of ε-caprolactone with dihydroxyl-terminated butadiene-*co*-acrylonitrile random copolymer was carried out in a living and controlled fashion. It should be pointed out that in the GPC experiment the molecular weights were measured by relating to PS equivalents and are unnecessarily the same as those measured with by ^{1}H NMR spectroscopy owing to the methodological difference. The molecular weights estimated by means of ^{1}H NMR spectroscopy were used throughout in this work.

3.2. Nanostructures in epoxy thermosets containing PCL-b-PBN-b-PCL

In the range of compositions investigated, all the thermosetting blends of epoxy with PCL-*b*-PBN-*b*-PCL were homogenous and

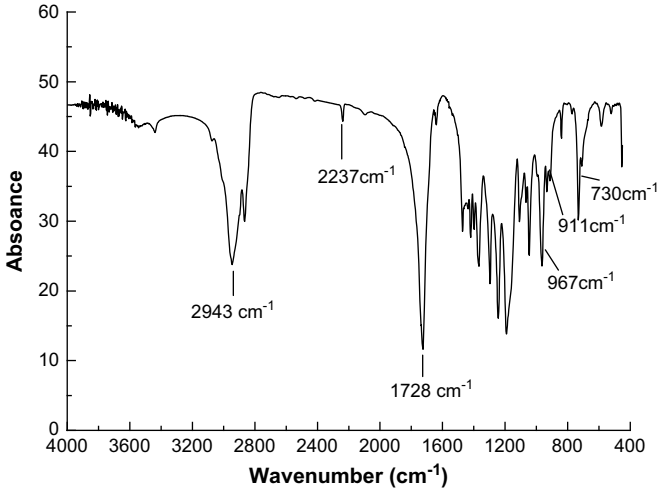

Fig. 1. FTIR spectrum of PCL-*b*-PBN-*b*-PCL triblock copolymer.

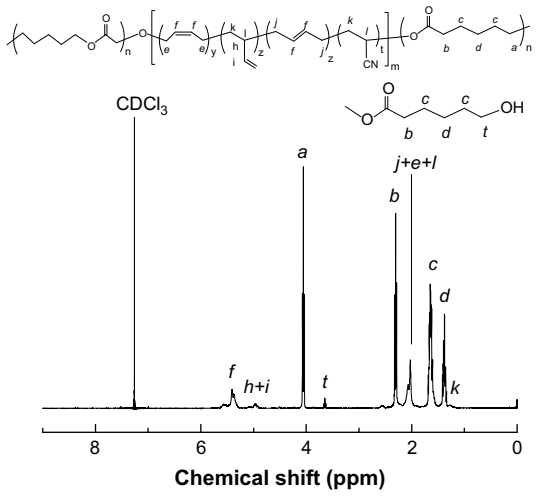

Fig. 2. ^{1}H NMR spectrum of PCL-*b*-PBN-*b*-PCL triblock copolymer.

transparent, indicating that no macroscopic phase separation occurred at least on the scale exceeding the wavelength of visible light. The morphologies of the thermosets were investigated by atomic force microscopy (AFM), transmission electronic microscopy (TEM) and small-angle X-ray scattering (SAXS) and, respectively. The AFM images of the thermosets containing 10, 20 and 30 of the triblock copolymer PCL-*b*-PBN-*b*-PCL are presented in Fig. 3. Shown in the left-hand side of each micrograph is the topography image and the right is the phase image. The topography images showed that the surfaces of the as-prepared specimens are free of visible defects and quite smooth and thus the effect of roughness resulting from the specimen trimming on morphology can be negligible. It is noted that all the blends exhibited nanostructured morphology. In terms of the volume fraction of PBN and the difference in viscoelastic properties between epoxy and PBN phases, the light continuous regions are ascribed to the epoxy matrix, which could be interpenetrated by the PCL blocks of the copolymer whilst the dark regions are attributed to PBN domains. It is observed that the spherical PBN nanoparticles with the size of 10–20 nm were homogenously dispersed into the continuous epoxy matrix and the sizes of the dispersed PBN particles increased with increasing the content of PCL-*b*-PBN-*b*-PCL in the thermosets (see Fig. 3A–C). The TEM micrographs of the thermosets containing 10, 20 and 30 wt% PCL-*b*-PBN-*b*-PCL are presented in Fig. 4. The heterogeneous morphology at the nanometer scale was observed in all the cases. The dark objects are assigned to PBN microphases since the PBN domains containing C=C double bonds can be preferentially stained with O_sO_4 whereas the epoxy matrix that is miscible with PCL was almost unaffected. For the thermoset containing 10 wt% PCL-*b*-PBN-*b*-PCL, the spherical PBN domains were dispersed in the continuous epoxy matrix with an average size of *ca.* 10 nm (Fig. 4A). The number of the spherical objects increased whereas the average distance between adjacent domains decreased with increasing the content of PCL-*b*-PBN-*b*-PCL in the thermosets. It is seen that the size of the nanoparticles almost remains invariant (see Fig. 4B). It is noted that when the content of PCL-*b*-PBN-*b*-PCL is 20 wt% or more, the spherical particles began to interconnect to some extent (Fig. 4C) and the thermosets possesses a combined morphology, in which both spherical PBN domains and some interconnected PBN domains were simultaneously present. When the content of PCL-*b*-PBN-*b*-PCL was increased up to 30 wt%, the domains of PBN were highly interconnected, forming interconnected objects at the nanometer scales. It should be pointed out that the micrographs of AMF are a little different from those obtained with TEM since the two techniques detect the information on phase behavior from different side views of structure. The latter are obtained on the basis of the difference in transmitted electronic densities through samples whereas the former reflects the information about tip-sample interactions resulting from adhesion [56], surface stiffness [57] and viscoelastic effects [58–60]. Therefore, the AFM results could be more sensitive to the transition region between PBN domain and the epoxy matrices that were interpenetrated by PCL chains. Nonetheless, the AFM experiments indeed indicate that the nanostructured epoxy thermosets were obtained. Shown in Fig. 5 are the SAXS profiles of the thermosets containing 10, 20 and 30 wt% PCL-*b*-PBN-*b*-PCL. The well-defined scattering peaks were observed in all the cases, indicating that the thermosets are microphase-separated. According to the position of the primary scattering peaks the average distance ($L = 2\pi/q_m$) between neighboring domains can be estimated to be 52.5, 36.1, 29.8 and 28.5 nm for the thermosets containing the block copolymer of 10, 20, 30 and 40 wt%, respectively. It is seen that the average distance between neighboring domains decreased with increasing the content of the triblock copolymer. These results are in a good agreement with those obtained by means of TEM.

It has been known that the formation of nanostructures in epoxy thermosets by the use of block copolymers could follow either self-assembly or reaction-induced microphase separation mechanism, depending on the miscibility of the subchains of the block copolymers with epoxy after and before curing reaction. Bates et al. [27,28] firstly reported the formation of the nanostructures in epoxy thermosets *via* self-assembly mechanism. The requirement of this approach is that precursors of epoxy act as the selective solvent for the block copolymers, *i.e.*, the block copolymers are self-organized into disordered or ordered micellar structures in their mixture with the precursors of epoxy prior to curing reaction and such self-assembled nanostructures are further fixed by initiating the polymerization of the precursor of epoxy. Therefore, self-assembly approach to nanostructures can be taken as a templating method although it has been noted that some minor structural changes could occur with the occurrence of curing reaction [27,28]. Recently, it is identified that reaction-induced microphase separation (RIMS) could be also involved with the formation of nanostructures in epoxy thermosets by the use of block copolymers [29,30]. In this approach, it is not required that the amphiphilic block copolymers are self-organized into the nanophases before curing reaction; all the subchains of block copolymers may be miscible with precursors of thermosets. Upon curing, only a part of subchains of block copolymers are demixed to form the nanostructured thermosets. In the present case, it is judged that the formation of the nanostructures in the epoxy thermosets containing PCL-*b*-PBN-*b*-PCL follows the reaction-induced phase separation rather than self-assembly mechanism in terms of the following knowledge: (i) that PCL is miscible with the epoxy after and before curing reaction [53,54] and (ii) that reaction-induced phase separation (RIPS) occurred in the thermosetting blends of epoxy with butadiene-*co*-acrylonitrile elastomer [1,3,5,9]. In this work, the miscibility of PCL blocks with epoxy matrix can be evidenced by differential scanning calorimetry (DSC) and Fourier transform infrared spectroscopy (FTIR). Shown in Fig. 6 are the DSC curves of PCL-*b*-PBN-*b*-PCL triblock copolymer and its thermosetting blends with epoxy thermosets. The pure triblock copolymer displayed an endothermic peak at 60 °C, which is assignable to the melting transition of PCL block. Nonetheless, it is noted that all the nanostructured thermosets containing the triblock did not exhibit the melting transition of PCL block, suggesting that the PCL blocks have been entrapped into the crosslinked networks of epoxy, *i.e.*, the PCL blocks remain miscible with epoxy matrix. In addition, the miscibility can be further confirmed by the fact that the glass transition

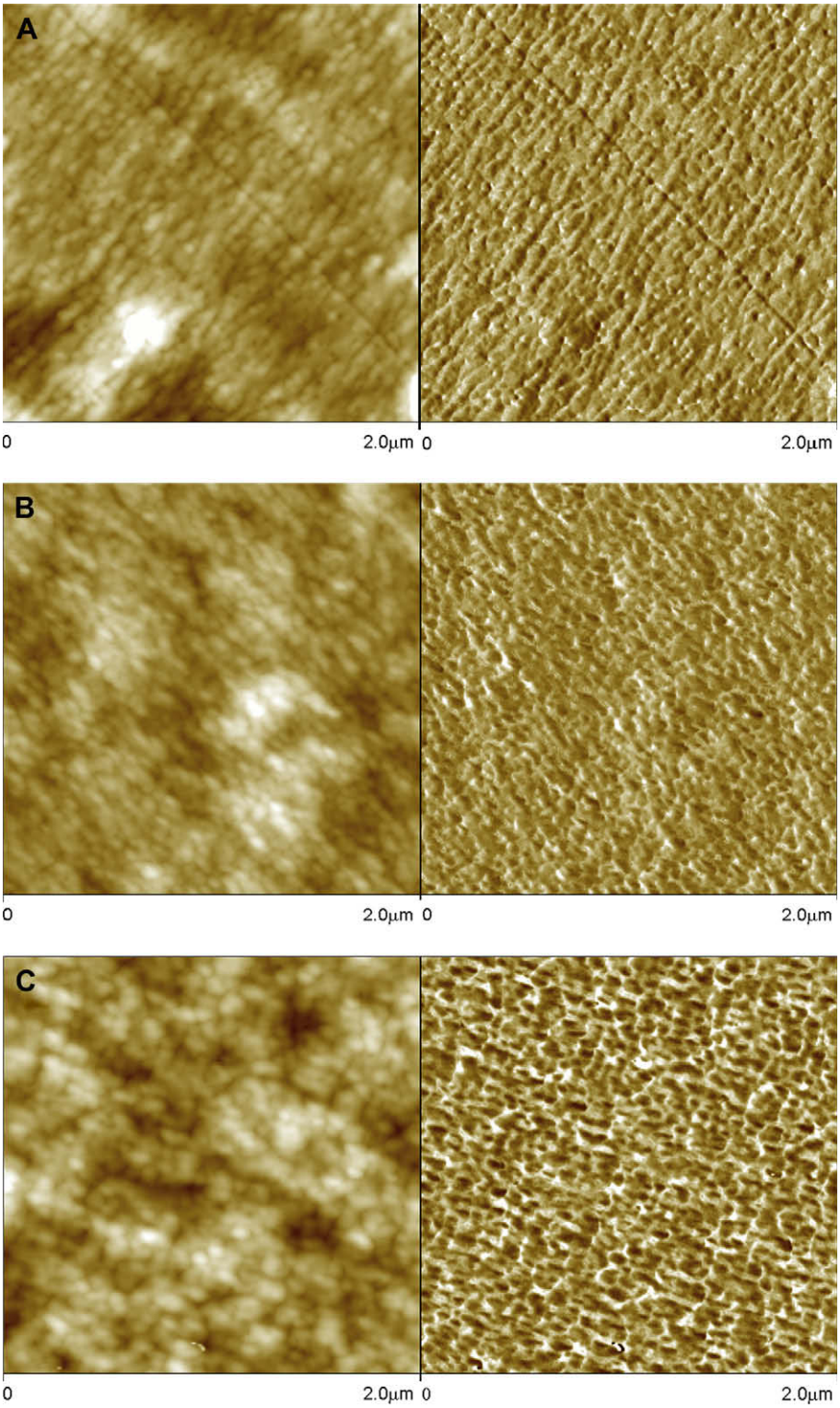

Fig. 3. AFM micrograph of the nanostructured epoxy containing: (A) 10 wt%; (B) 20 wt%; (C) 30 wt% PCL-*b*-PBN-*b*-PCL triblock copolymer.

temperatures (T_gs) of the matrices deceased with increasing the content of PCL-*b*-PBN-*b*-PCL triblock copolymer. The miscibility of PCL blocks with amine-cured epoxy is ascribed to the formation of the intermolecular hydrogen-bonding interactions between carbonyl groups of PCL and secondary hydroxyl groups of epoxy thermosets. Shown in Fig. 7 are the FTIR spectra of PCL-*b*-PBN-*b*-PCL and the nanostructured thermosets containing PCL-*b*-PBN-*b*-PCL in the range of 1680–1800 cm^{-1}. The absorption band in this range is ascribed to the stretching vibration of carbonyl groups. For the PCL-*b*-PBN-*b*-PCL at the room temperature, it is seen that the FTIR spectrum is composed of two components. The one component at 1735 cm^{-1} is assignable to the amorphous chains of PCL while another at 1725 cm^{-1} is ascribed to the carbonyls in the crystalline region of PCL. In the nanostructured thermosets, it is

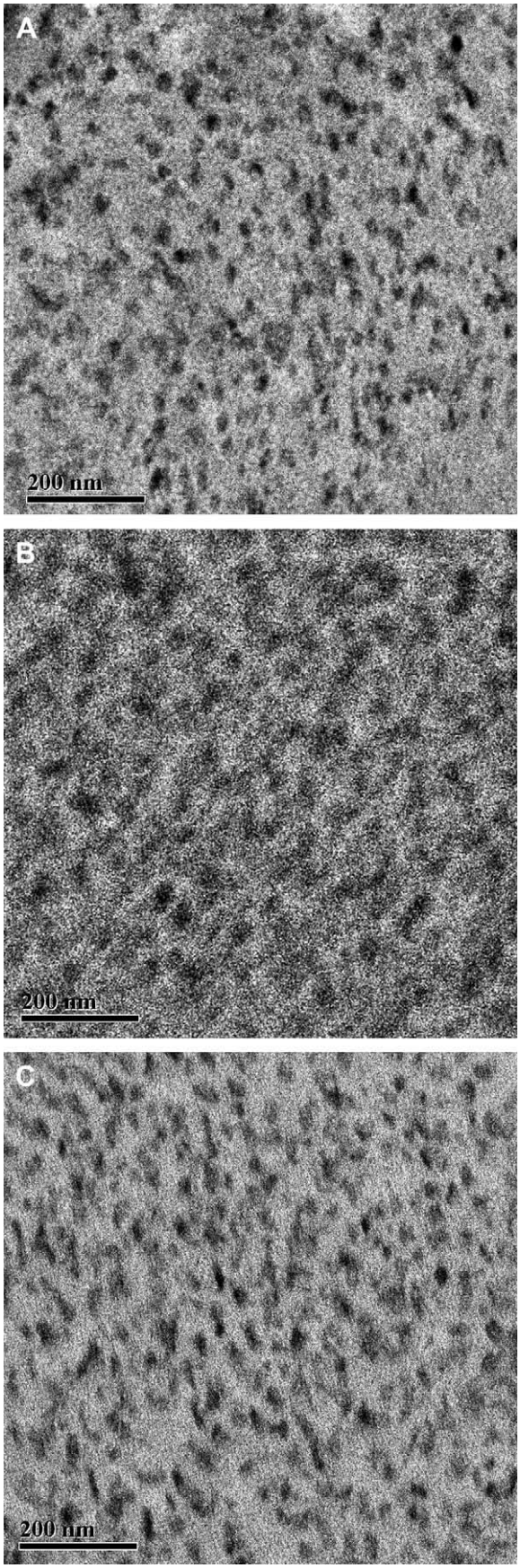

Fig. 4. TEM micrograph of the nanostructured epoxy containing: (A) 10 wt%; (B) 20 wt%; (C) 30 wt% PCL-*b*-PBN-*b*-PCL triblock copolymer.

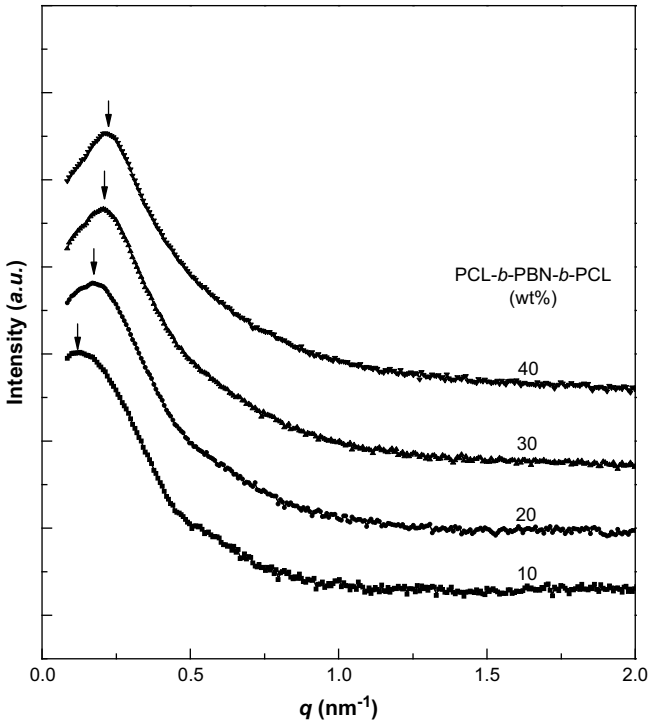

Fig. 5. SAXS profiles of the nanostructured epoxy containing PCL-*b*-PBN-*b*-PCL triblock copolymer.

noted that the band assignable to crystalline region of PCL disappeared; instead the new shoulder bands at the lower frequency (1706 cm^{-1}) appeared. The shoulder band is ascribed to the stretching vibration of the carbonyl groups which are hydrogen bonded with the secondary hydroxyl groups of MOCA-cured epoxy resins. In addition, it is noted that the band at 1731 cm^{-1} shifted to the higher frequency 1734 cm^{-1} with increasing the concentration

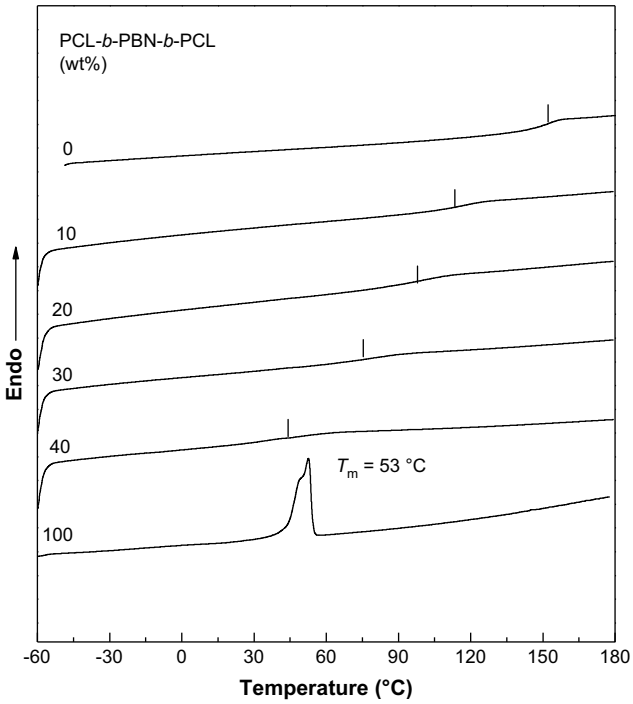

Fig. 6. DSC curves of the nanostructured epoxy thermosets.

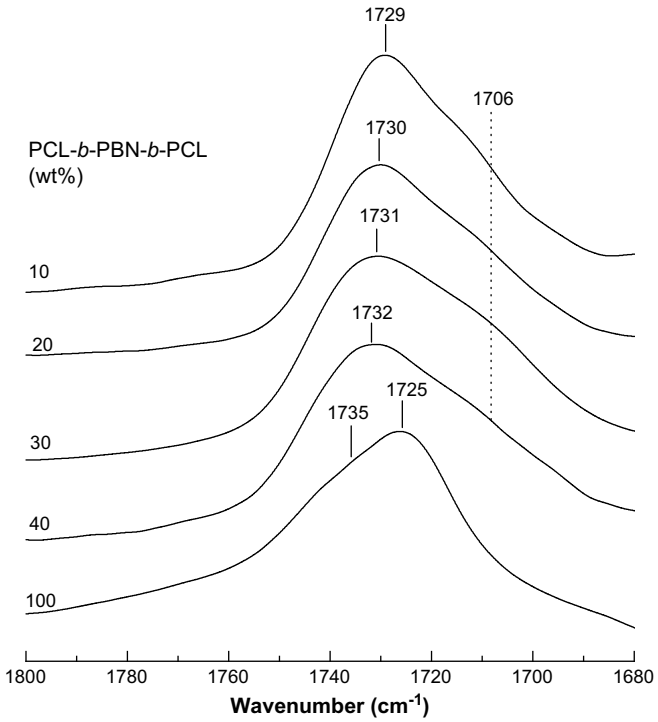

Fig. 7. FTIR spectra of the nanostructured thermosets in the range of 1680–1800 cm^{-1}.

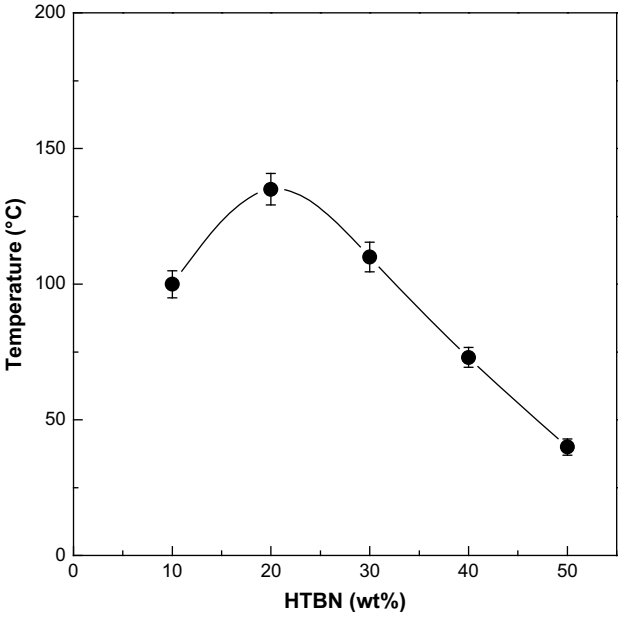

Fig. 8. Cloud point curve of DGEBA/HTBN mixtures.

of the triblock copolymer. The FTIR results indicated that the intermolecular hydrogen-bonding interactions were formed between the carbonyl of PCL subchains and the hydroxyl groups of crosslinked epoxy. For the thermosetting blend of epoxy resin with the PBN identical with those of the subchains of the triblock copolymer in the nanostructured thermosets, it was observed that all the mixtures composed of the precursors of epoxy and HTBN are cloudy at room temperature before curing reaction. Upon heating up to *ca.* 120 °C, the mixtures became homogenous and transparent, suggesting that the mixtures displayed an upper critical solution temperature behavior (UCST). By using phase contrast microscopy equipped a hot stage, the cloud point curve of the DGEBA/HTBN blends was determined as shown in Fig. 8. An asymmetrical phase diagram was obtained and the mixture exhibited the highest critical solution temperature at 120 °C while the concentration of HTBN is about 20 wt%. It should be pointed out that with adding the curing agent (*viz.* MOCA) to the binary mixtures of DGEBA and PBN, the ternary mixtures became completely homogenous and transparent even at room temperature, suggesting that the UCST phase behavior disappeared, *i.e.*, the ternary mixtures composed of DGEBA, MOCA and PBN are totally miscible. The ternary mixtures were subjected to curing reaction at 150 °C for 4 h to obtain the thermosetting blends. It is observed that with the curing reaction proceeding at the elevated temperature, the initial transparent system gradually became cloudy, indicating the occurrence of the reaction-induced phase separation.

In marked contrast to the epoxy thermosets containing PCL-*b*-PBN-*b*-PCL triblock copolymer, the ternary blends of epoxy with PBN and the model PCL having the identical molecular weight of with the length of PCL block in the block copolymer displayed the heterogeneous morphology at the micrometer scale. The morphology of ternary thermosetting blends was investigated by means of electronic scanning microscopy (SEM). The SEM micrographs are shown in Fig. 9. The specimens for the morphological observation were prepared *via* fracturing the blends under cryogenic conditions using liquid nitrogen. The SEM shows that all the blends displayed the heterogeneous morphology. For the epoxy containing the modifier (PBN + 2PCL) of 10 wt%, the spherical particles at the size of 3–5 μm in diameter were uniformed dispersed in the continuous matrix and the average size of the spherical particle increases with increasing PBN content. The spherical particles were attributed to PBN phase whereas the continuous matrices were ascribed to the miscible blends composed of the crosslinked epoxy and PCL since PCL is miscible with the aromatic amine-crosslinked epoxy. With the identical compositions, the ternary blends are compared to the nanostructured thermosets to indicate the effect of the formation of the nanostructures on the thermal and mechanical properties of the materials.

3.3. Thermal and mechanical properties

3.3.1. Glass transition temperatures

The nanostructured thermosets containing PCL-*b*-PBN-*b*-PCL triblock copolymer were subjected to dynamic mechanical thermal analysis (DMTA) and the dynamic mechanical spectra are shown in Fig. 10. The control epoxy thermoset exhibited a well-defined relaxation peak (*i.e.*, α transition) centered at *ca.* 160 °C, which is responsible for the glass–rubber transition of the crosslinked polymer. Apart from the α transition, the aromatic amine-cured epoxy exhibited a secondary transition (*i.e.*, β transition) at the lower temperatures (approximately −60 °C). The transition are attributed predominantly to the motion of hydroxyl ether [–CH_2–CH(OH)–CH_2–O–] structural units in amine-crosslinked epoxy (see Fig. 10A) [61–63]. Apart from the α and β transitions, there are a secondary transition at *ca.* 75 °C, which could be ascribed to the motion of diphenyl structural units of the epoxy networks [61–63]. Upon adding PCL-*b*-PBN-*b*-PCL into the thermosets, the α transition shifted to the lower temperatures. The T_gs of the epoxy matrix decreased with increasing the content of PCL-*b*-PBN-*b*-PCL triblock copolymer. The decreased T_gs are ascribed to the plasticization of PCL subchains of the triblock copolymer on the epoxy matrix. It is noted that the α peak (*i.e.*, glass transition) of PBN microphase is not disenable until the concentration of PCL-*b*-PBN-*b*-PCL triblock copolymer is 30 wt% or higher and is situated at −48 °C. The intensity of this transition increased with increasing the content of

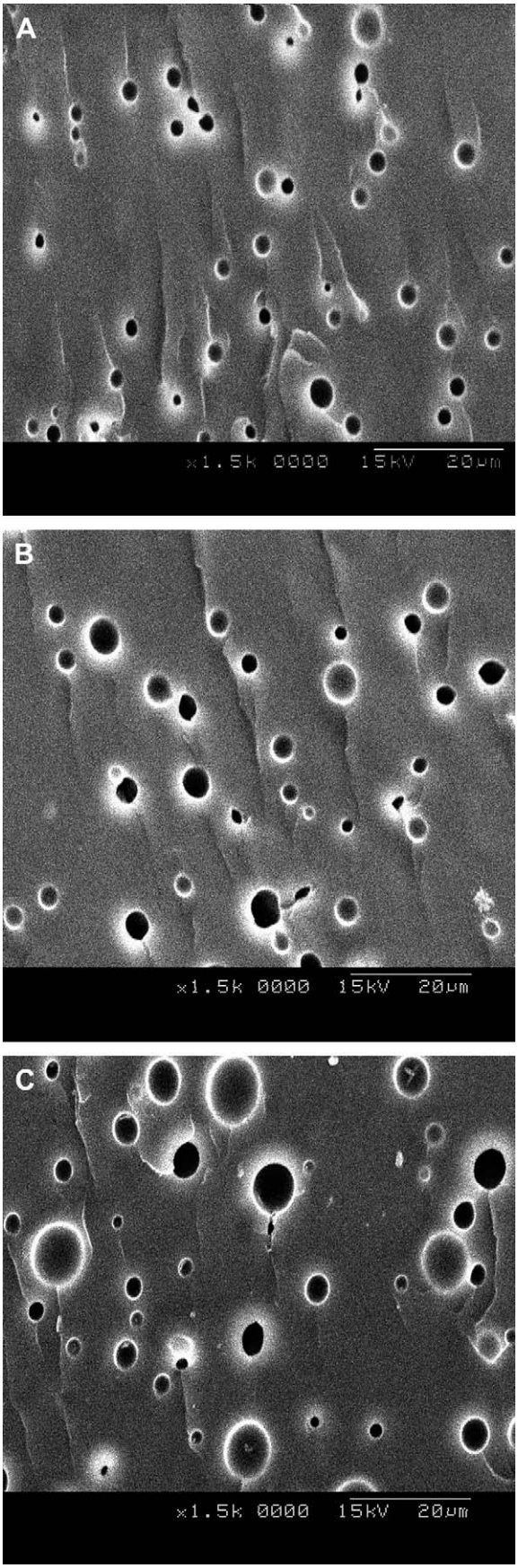

Fig. 9. SEM micrograph of the ternary blends containing (A) 10 wt%; (B) 20 wt%; (C) 30 wt% (HTBN + 2PCL).

the triblock copolymer. For comparison, the DMA curves of the ternary thermosets composed of epoxy, PBN and PCL with the identical compositions were also incorporated in Fig. 10B–E. In all the DMA spectra of the ternary blends, the α and β transitions of epoxy matrix are similarly exhibited as in the nanostructured thermosets. The glass transition of PBN-rich phase is discernible when the concentration of PBN + 2PCL is 30 wt% or higher. It is noted that with the identical composition, the T_gs of the epoxy matrix for the nanostructured blends are significantly higher than those of the ternary blends. When the content of the modifier is 40 wt% or higher, the rubbery plateau of storage modulus cannot be measured for the ternary blends of epoxy, PBN and PCL under the present condition, implying that a phase-inversion occurred for the blend. In contrast, the nanostructured thermosets containing 40% PCL-*b*-PBN-*b*-PCL can display a well-defined rubbery plateau of storage modulus in the dynamic mechanical measurements. In addition, it is noted that the storage moduli of the nanostructured thermosets are lower than those of the ternary thermosets with the identical contents of the modifier when the content of the modifiers is more than 10 wt%.

The formation of nanostructures in the epoxy thermosets containing PCL-*b*-PBN-*b*-PCL triblock copolymer has a profound impact on the glass transition behavior of the thermosets compared to the ternary blends composed of epoxy, PCL and HTBN. The dynamic mechanical analysis has shown that with the identical concentrations of the modifiers (*i.e.*, PCL-*b*-PBN-*b*-PCL and HTBN + PCL) the nanostructured thermosets significantly displayed the higher T_gs than the ternary thermosets. It is plausible to propose that the following factors result in the difference in T_gs between the ternary blends and the nanostructured blends. Firstly, the increased T_gs for the triblock copolymer-containing blends could be associated with the formation of the nanostructures in the thermosets. In the nanostructured thermosets, the PCL chains have to be enriched at the surface of the microphase-separated PBN nanodomains due to the presence of chemical bonds between PBN and PCL blocks. Owing to the steric hindrance, the PCL blocks at the intimate surface of PBN nanodomains were unable completely to mix with epoxy matrix, *i.e.*, the less PCL chains were interpenetrated with the epoxy matrix in the nanostructured thermosets. Therefore, the plasticization of PCL chains on the epoxy matrix would be effectively reduced, which causes the increased T_gs of epoxy matrix. By means of small-angle X-ray scattering (SAXS), Hillmyer et al. [32] reported the demixing phenomenon of the miscible block in the thermosetting blends of epoxy with PEO-*b*-PEE diblock copolymer due to the occurrence of curing reaction; the formation of nanostructures in this system was demonstrated to follow a self-assembly mechanism. In the present system, the formation of the nanostructures is responsible for reaction-induced microphase separation and the demixing behavior was well identified in views of glass transition behavior. In marked contrast to the nanostructured blends, the PCL chains were homogeneously dispersed into the epoxy matrix and were well interpenetrated into the crosslinked epoxy networks *via* the formation of the intermolecular hydrogen-bonding interactions in the ternary thermosetting blends and thus the epoxy matrix was well plasticized by the free PCL chains. Secondly, the lower T_gs of the matrix for the ternary blends could be additionally ascribed to the presence of the more ends of polymeric chains (*i.e.*, PCL). The more free ends of chains the more free volume will be introduced into the system and thus the lower T_gs of the matrix are displayed.

3.3.2. Fracture toughness

The fracture toughness of the nanostructured thermosets containing PCL-*b*-PBN-*b*-PCL triblock copolymer was evaluated in

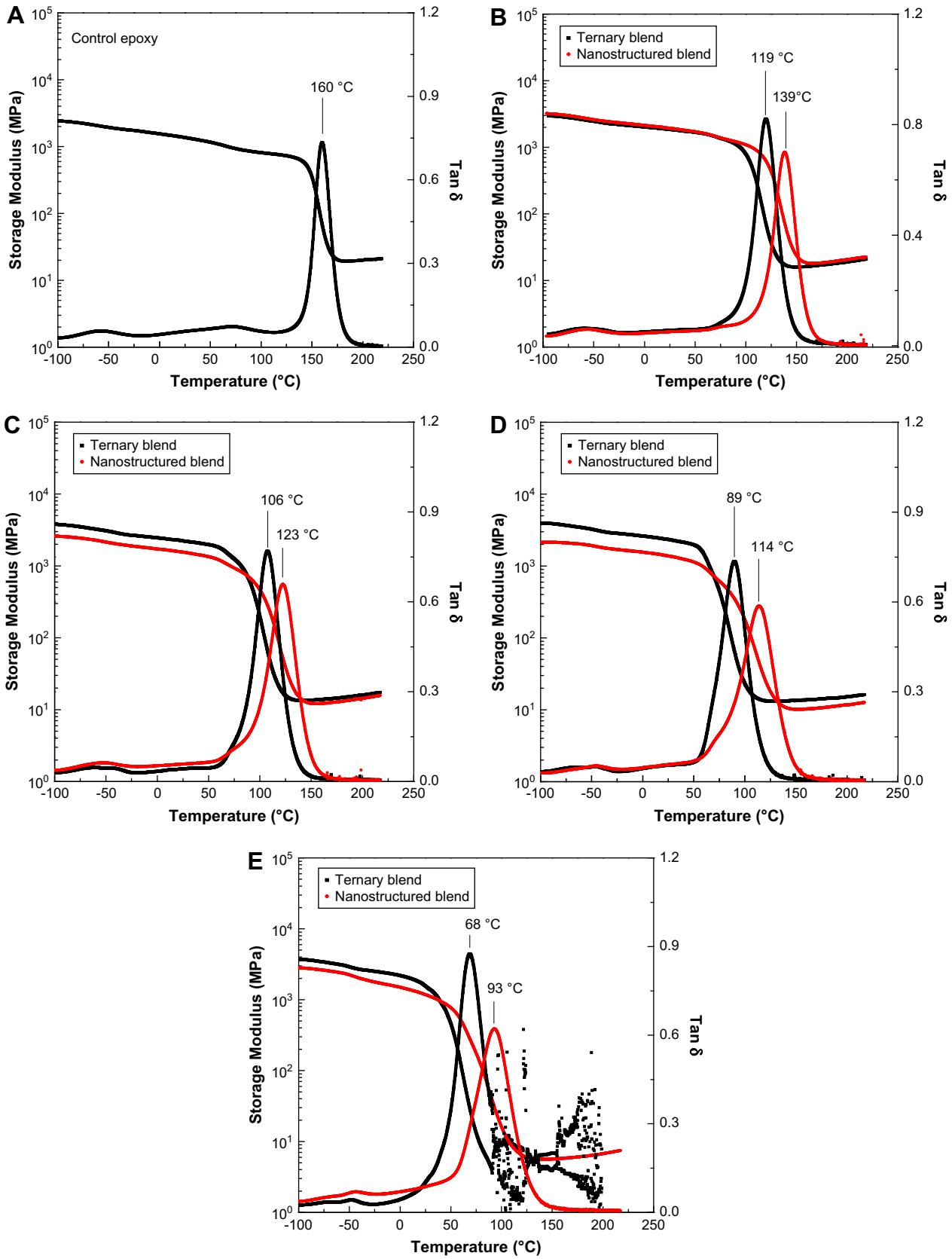

Fig. 10. DMA curves of the control epoxy, ternary blends and the nanostructured thermosets containing PCL-*b*-PBN-*b*-PCL: (A) control epoxy, (B) 10 wt%; (C) 20 wt%; (D) 30 wt% and (E) 40 wt% modifiers (*i.e.*, HTBN + 2PCL and/or PCL-*b*-PBN-*b*-PCL).

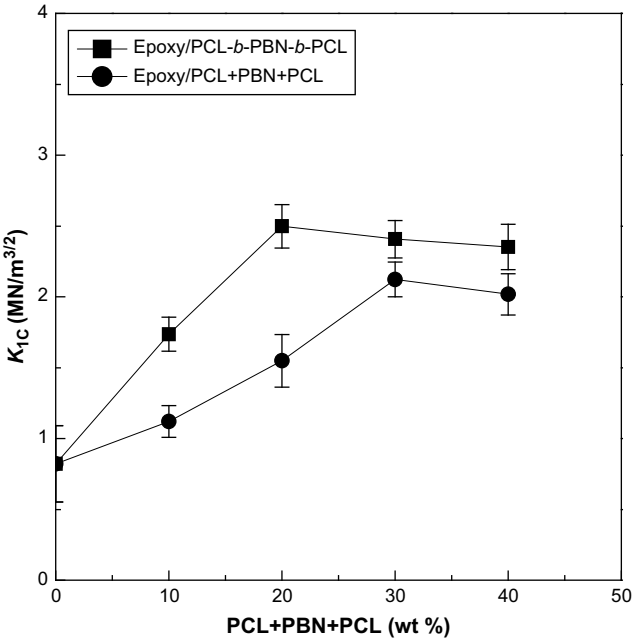

Fig. 11. Plots of K_{1C} as function of modifiers for the nanostructured epoxy thermosets containing PCL-*b*-PBN-*b*-PCL triblock copolymer and ternary blends of epoxy, HTBN and PCL.

terms of three-point bending tests to measure the critical stress intensity factor (K_{1C}). In the meantime, the fracture toughness of the ternary thermosetting blends composed of epoxy, PBN and PCL was also measured. The plots of K_{1C} as a function of the content of PCL + PBN for the thermosets are presented in Fig. 11. The content of PBN + PCL in the ternary thermosetting blends is controlled to be identical with that of the nanostructured thermosets. It is seen that the K_{1C} values of all the thermosetting blends are higher than that of the control epoxy, indicating that the epoxy thermoset was significantly toughened with the inclusions of the modifiers (*i.e.*, PCL-*b*-PBN-*b*-PCL and/or HTBN + PCL). The values of K_{1C} increased with increasing the content of the modifiers. For the nanostructured thermosets containing PCL-*b*-PBN-*b*-PCL triblock copolymer, the value of K_{1C} attains its maximum (*i.e.*, 1.98 MN/m$^{3/2}$) while the concentration of the triblock copolymer is 20 wt%. The K_{1C} value is more than the twice as that of the control epoxy thermoset ($K_{1C} = 0.8$ MN/m$^{3/2}$). In contrast, the value of K_{1C} did not attain the maximum until the concentration of modifier (*i.e.*, HTBN + PCL) reached 30 wt% for the ternary blends and the maximum of the K_{1C} is 1.6 MN/m$^{3/2}$. It is worth noticing that with the identical content of the modifier the values of K_{1C} for the nanostructured thermosets containing the triblock copolymer are significantly higher than those of the ternary blends. In another word, the fracture toughness of the nanostructured blends is much higher than that of the ternary blends with the identical content of modifiers.

Toughness improvement of epoxy thermosets with liquid rubbers has been extensively investigated during the past decades. As the model system, the liquid rubbers such as carboxyl (or amino)-terminated butadiene-*co*-acrylonitrile rubber (CTBN or ATBN) have been used to toughen epoxy resin [2,3,64–66]. It is recognized that a combination of cavitation around the rubber particles with shear yielding in the matrix plays a major role in providing mechanism for energy dissipation [38,51–53]. In addition, microvoiding and tearing of the rubber particles may also occur. Compared to the thermosets modified with the liquid rubber, which possess the phase-separated morphology at the micrometer scale, the toughness improvement of the thermosets *via* the formation of the nanostructures could display the following features: (i) the elastomeric component (*viz.* PBN rubber) was homogenously dispersed in the thermosetting matrix at the nanometer scale, which will greatly optimize the interactions between the thermosetting matrix and the modifier; (ii) the interface interactions between thermosetting matrix and the PBN nanodomains was significantly increased due to the miscibility of PCL blocks with the epoxy thermosets. Therefore, the toughness improvement for the nanostructured blends involving epoxy and PCL-*b*-PBN-*b*-PCL triblock copolymer is much higher than that of the ternary blends of epoxy, PBN and PCL. In addition, the effect of the nanostructures on the toughness improvement is reflected by the smaller loading of the modifier than the ternary blends. It has been proposed that toughening of thermosets *via* the formation of nanostructures are quite dependent on type and shape of dispersed microdomains and the mechanisms could involving either the debonding of micelles (or vesicles) from epoxy matrix or crack deflection and frictional interlocking for the thermosets possessing the terraced morphology [36]. In the present case, the wormlike nanophases of PBN were obtained when the concentration of PCL-*b*-PBN-*b*-PCL triblock copolymer is 20 wt% or higher and thus the energy-dissipation mechanisms could be related on the specific nanostructures of epoxy thermosets modified with the triblock copolymer. Nonetheless, the correlations between toughening mechanisms and nanostructures of thermosets containing block copolymers remains largely unexplored vis-à-vis those for elastomers (and/or thermoplastic)-modified thermosets.

4. Conclusions

Poly(ε-caprolactone)-*block*-poly(butadiene-*co*-acrylonitrile)-*block*-poly(ε-caprolactone) triblock copolymer was synthesized and incorporated into epoxy thermosets. The nanostructures of the thermosetting blends were investigated by means of transmission electronic microscopy (TEM), atom force microscopy (AFM) and small-angle X-ray scattering (SAXS). The formation of the nanostructures in the thermosetting composites was judged to follow reaction-induced microphase separation in terms of the difference in miscibility of poly(butadiene-*co*-acrylonitrile) and poly(ε-caprolactone) subchains with epoxy resin after and before curing reaction. The thermal properties of the nanostructured thermosetting blends were compared with those of the ternary blends of epoxy resin comprised of poly(butadiene-*co*-acrylonitrile) and poly(ε-caprolactone). It is noted that the nanostructured thermosetting blends displayed higher glass transition temperatures (T_gs) than the binary blends with the identical composition, which was evidenced by dynamic mechanical analysis. The fracture toughness of the nanostructured blends was evaluated in term of the measurement of stress field intensity factor (K_{1C}) of the thermosetting blends of epoxy resin with the modifiers. It is identified that with the identical composition the nanostructured blends displayed higher fracture toughness than the ternary blends. With the less content of the modifier the nanostructures gave the maximum K_{1C}.

Acknowledgments

The financial supports from Natural Science Foundation of China (Nos. 20474038 and 50873059) and National Basic Research Program of China (No. 2009CB930400) are acknowledged. The authors thank Shanghai Leading Academic Discipline Project (Project Number: B202) for the partial support.

References

[1] Bauer RS, editor. Epoxy resin chemistry II: ACS symposium series, no. 221. Washington, DC: American Chemical Society; 1983.
[2] Riew CK, Gillham JK, editors. Rubber-modified thermoset resins, Advances in chemistry series 208. Washington, DC: American Chemical Society; 1989.
[3] Riew CK, Kinloch AJ, editors. Toughened plastics I: science and engineering, ACS series no. 233. Washington, DC: American Chemical Society; 1993.
[4] Kinloch AJ, Shaw SJ, Tod DA, Hunston DL. Polymer 1983;24:1355.
[5] Yee AF, Pearson RA. J Mater Sci 1986;21:2462.
[6] Yorkgitis EM, Eiss NS, Tran C, Wilkes GL, McGrath LE. Am Chem Soc Adv Polym Sci 1985;72:70.
[7] Meijerink JI, Eguchi S, Ogata M, Ishii T, Amagi S, Numata S, et al. Polymer 1994;35:179.
[8] Kemp TJ, Wilford A, Howarth OW, Lee TCP. Polymer 1992;33:1860.
[9] Hisich HS-Y. Polym Eng Sci 1990;30:493.
[10] Bussi P, Ishida H. J Appl Polym Sci 1994;32:647.
[11] Bucknall CB, Patridge IK. Polymer 1983;24:639.
[12] Bucknall CB, Gilbert AH. Polymer 1989;30:213.
[13] Hourston DJ, Lane JM. Polymer 1992;33:1397.
[14] Hedrick JH, Yilgor I, Jurek M, Hedrick JC, Wilkens GL, McGrath JE. Polymer 1991;13:2020.
[15] Raghava RS. J Polym Sci Part B Polym Phys 1988;26:65.
[16] Gilbert AH, Bucknall CB. Macromol Chem Phys Macromol Symp 1991; 45:289.
[17] Cho JB, Hwang JW, Cho K, An JH, Park CE. Polymer 1993;34:4832.
[18] Zheng S, Wang J, Guo Q, Wei J, Li J. Polymer 1996;37:4667.
[19] Takahashi T, Nakajima N, Saito N. In: Riew CK, editor. Rubber-toughened plastics, Advances in chemistry series 222. Washington, DC: American Chemical Society; 1989. p. 243.
[20] Pascault JP, Williams RJJ. In: Paul DR, Bucknall CB, editors. Polymer blends, vol. 1. New York: Wiley; 2000. p. 379–415.
[21] Kinloch AJ, Yong RJ. Fracture behavior of polymers. London and New York: Applied Science Publishers Ltd.; 1983.
[22] Sigl LS, Mataga PA, Dageleidsh BI, McKeeking RM, Evans AG. Acta Metall 1988;36:945.
[23] Lange FF. J Mater Sci 1971;54:983.
[24] Evans AG, Williams S, Beaumont PWR. J Mater Sci 1985;20:3668.
[25] Oritz MJ. Appl Mech 1987;54:54.
[26] Ruiz-Perez L, Royston GJ, Fairclough JP, Pyan AJ. Polymer 2008;49:4475.
[27] Hillmyer MA, Lipic PM, Hajduk DA, Almdal K, Bates FS. J Am Chem Soc 1997;119:2749.
[28] Lipic PM, Bates FS, Hillmyer MA. J Am Chem Soc 1998;120:8963.
[29] Mijovic J, Shen M, Sy JW, Mondragon I. Macromolecules 2000;33:5235.
[30] Grubbs RB, Dean JM, Broz ME, Bates FS. Macromolecules 2000;33:9522.
[31] Kosonen H, Ruokolainen J, Nyholm P, Ikkala O. Macromolecules 2001;34:3046.
[32] Guo Q, Thomann R, Gronski W. Macromolecules 2002;35:3133.
[33] Ritzenthaler S, Court F, Girard-Reydet E, Leibler L, Pascault JP. Macromolecules 2002;35:6245.
[34] Ritzenthaler S, Court F, Girard-Reydet E, Leibler L, Pascault JP. Macromolecules 2003;36:118.
[35] Rebizant V, Abetz V, Tournihac T, Court F, Leibler L. Macromolecules 2003; 36:9889.
[36] Dean JM, Verghese NE, Pham HQ, Bates FS. Macromolecules 2003;36:9267.
[37] Rebizant V, Venet AS, Tournillhac F, Girard-Reydet E, Navarro C, Pascault JP, et al. Macromolecules 2004;37:8017.
[38] Zucchi IA, Galante MJ, Williams RJJ. Polymer 2005;46:2603.
[39] Thio YS, Wu J, Bates FS. Macromolecules 2006;39:7187.
[40] Maiez-Tribut S, Pascault JP, Soulé ER, Borrajo J, Williams RJJ. Macromolecules 2007;40:1268.
[41] Gong W, Zeng K, Wang L, Zheng S. Polymer 2008;49:3318.
[42] Meng F, Zheng S, Zhang W, Li H, Liang Q. Macromolecules 2006;39:711.
[43] Serrano E, Tercjak A, Kortaberria G, Pomposo JA, Mecerreyes D, Zafeiropoulos NE, et al. Macromolecules 2006;39:2254.
[44] Meng F, Zheng S, Li H, Liang Q, Liu T. Macromolecules 2006;39:5072.
[45] Meng F, Zheng S, Liu T. Polymer 2006;47:7590.
[46] Sinturel C, Vayer M, Erre R, Amenitsch H. Macromolecules 2007;40:2532.
[47] Ocando C, Serrano E, Tercjak A, Pena C, Kortaberria G, Calberg C, et al. Macromolecules 2007;40:4068.
[48] Xu Z, Zheng S. Macromolecules 2007;40:2548.
[49] Meng F, Xu Z, Zheng S. Macromolecules 2008;41:1411.
[50] Dean JM, Grubbs RB, Saad W, Cook RF, Bates FS. J Polym Sci Part B Polym Phys 2003;41:2444.
[51] Wu J, Thio YS, Bates FS. J Polym Sci Part B Polym Phys 2005;43:1950.
[52] Dean JM, Lipic PM, Grubbs RB, Cook RF, Bates FS. J Polym Sci Part B Polym Phys 2001;39:2996.
[53] Yin M, Zheng S. Macromol Chem Phys 2005;206:929.
[54] Ni Y, Zheng S. Polymer 2005;46:5828.
[55] Tanaka H, Nishi T. Phys Rev A 1989;39:783.
[56] Schmitz I, Schreiner M, Friedbacher G, Grasserbauer M. Appl Surf Sci 1997; 115:190.
[57] Magonov SN, Elings V, Whangbo MH. Surf Sci 1997;375:L385.
[58] Tamayo A, Garcia R. Langmuir 1996;12:4434.
[59] Chen X, McGurk SL, Davies MC, Roberts CJ, Shakesheff KM, Davies J, et al. Macromolecules 1998;31:2278.
[60] Clarke S, Davies MC, Roberts CJ, Tendler SJB, Williams PM, Lewis AL, et al. Macromolecules 2001;34:4166.
[61] Sanja ZN, Kupehela L. Polym Eng Sci 1976;28:1149.
[62] Ochi M, Okasaki M, Shimbo M. J Polym Sci Part B Polym Phys 1982;20:89.
[63] Shibanov YD, Godovsky YK. Prog Colloid Polym Sci 1989;80:110.
[64] Pearson RA, Yee AF. J Mater Sci 1986;21:2475.
[65] Pearson RA, Yee AF. J Mater Sci 1989;24:2571.
[66] Thomas R, Abraham J, Thomas PS, Thomas S. J Polym Sci Part B Polym Phys 2004;42:2531.